J Electroceram (2011) 27:33–37
DOI 10.1007/s10832-011-9646-7

# Electrical and optical characterisation of aluminium nitride piezoelectric films on silicon nitride membranes

**Didier Cornez · Jocelyn Elgoyhen · David Hutson · Cecile Percier · Perrine Plissard · Mark Begbie · Aboubacar Chaehoi · Katherine J. Kirk**

Received: 23 September 2008 / Accepted: 1 June 2011 / Published online: 14 June 2011
© Springer Science+Business Media, LLC 2011

**Abstract** Aluminium nitride (AlN) is a thin film piezoelectric material having excellent potential for integration with microelectronic systems. We have investigated flexural modes of $Si_3N_4$ membrane structures with and without an AlN active layer. AlN films typically 3 μm thick were deposited by RF sputtering. Mechanical excitation was provided acoustically by sweeping the excitation frequency of a 1 MHz air-coupled ultrasonic transducer. Mode shapes were verified by scanning laser vibrometry up to the [3,3] mode, in the frequency range 100 kHz to 1 MHz. Resonant frequencies were identified at the predicted values provided the tension in the layers could be estimated. For a membrane structure incorporating an AlN layer, acoustic and electrical excitation of flexural modes was confirmed by displacement measurements using laser vibrometry and resonant frequencies were compared with analytical calculations.

**Keywords** MEMS · Aluminium nitride · Flexural modes · Thin film piezoelectric

## 1 Introduction

Thin membranes of $Si_3N_4$ fabricated as “windows” in a silicon substrate have been extensively used to provide a support to complex structures such as micro-electro-mechanical systems (MEMS) in applications such as sensors, actuators or transducers [1–4]. Thus understanding the behaviour of the base support of the composite structure becomes a requirement when it is necessary to control the physical deformation of the system, for example for energy harvesting [5].

We are interested in using aluminium nitride (AlN) thin films as an electro-mechanically active layer in MEMS. AlN is a piezoelectric material which is convenient to deposit as a thin film and does not require the high temperature processing (600–900°C) required for films of poled ferroelectric ceramics such as PZT ($PbZr_{1-x}Ti_xO_3$). In addition, AlN retains its properties under processing temperatures commonly used in CMOS (200–400°C), giving advantages for integration and manufacturability. Set against these advantages is the small size of the piezoelectric strain coefficient $d_{33}$ which is much lower for AlN (5.0 pC $N^{-1}$) than for bulk PZT (200–600 pC $N^{-1}$) and is more comparable to other non-ferroelectric crystalline materials such as quartz.

In this work we used scanning laser vibrometry to characterise the flexural modes of membrane structures with and without AlN and compared the results with analytical calculations. We also characterised electrically and acoustically devices incorporating a piezoelectric AlN thin film as an active layer in a MEMS structure.

## 2 Device structure and flexural modes

Flexural mode shapes and frequencies were calculated using an analytical approach based on simple resonance modes of a square membrane [6]. The deflection of a stretched membrane under an external load follows the

D. Cornez · J. Elgoyhen · D. Hutson · C. Percier · P. Plissard · K. J. Kirk (✉)
Microscale Sensors, School of Engineering, University of the West of Scotland, Scotland PA1 2BE, UK
e-mail: katherine.kirk@uws.ac.uk

M. Begbie · A. Chaehoi
Institute for System Level Integration, Alba Centre, Alba Campus, Livingston EH54 7EG, UK

Poisson equation, which has standing wave solutions for displacement $U(x,y,t)$

$$U(x,y,t)=\begin{cases} \sin(k_m x)\sin(k_n y)\sin(2\pi v_{m,n}t)\begin{cases}0<x<x_0\\0<y<y_0\end{cases} \\ 0\begin{cases}x\leq 0\\x\geq x_0\\y\leq 0\\y\geq y_0\end{cases}\end{cases} \quad (1)$$

where $x_0 = y_0$ is the side length of the square. In this case the system is a homogeneous $Si_3N_4$ membrane stretched across a square opening in a silicon substrate such that its outer edges are clamped at the rim. Therefore the boundary conditions shown in Eq. 1 apply, with zero displacement outside the membrane area.

The membrane has density per unit area, μ, and tension per unit length, *T.* Because the membrane is square, the frequency [7] can be simply expressed in terms of the mode of vibration [*m*, *n*] as:

$$f_{m,n}=\frac{1}{2l}\sqrt{\frac{T}{\mu}(m^2+n^2)} \quad (2)$$

where *l* is the side length of the membrane, and *m* and *n* are integers. As the membrane size decreases the fundamental flexural mode resonant frequency increases.

Three different $Si_3N_4$ membrane-based samples were used in this investigation: a rather large 3.6×3.6 $mm^2$ 200 nm thick $Si_3N_4$ membrane, a smaller 400×400 $\mu m^2$ 300 nm thick $Si_3N_4$ membrane patterned with a piezoresisistive “pressure sensor” device structure, and the same pressure sensor structure with an AlN film and electrodes added as shown in Fig. 1.

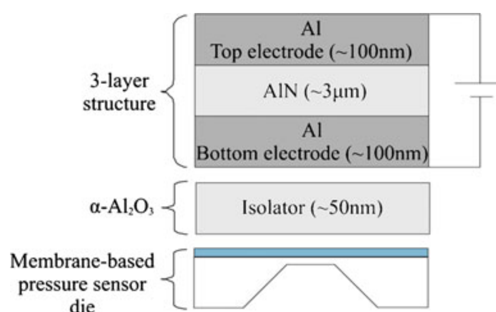


**Fig. 1** Schematic representation of membrane structure incorporating AlN layer. Size of the Si pressure sensor die was 5×5 $mm^2$ with 300 nm thick $Si_3N_4$ membrane

Materials parameters are given in Table 1 for the $Si_3N_4$ membrane, electrodes, and active layers. The effect of the very thin (50 nm) alumina isolator layer shown in Fig. 1 was regarded as negligible in the analysis. Properties of the $Si_3N_4$ membrane were assumed to be typical values for low stress nitride deposited by the LPCVD process. The value of the density per unit area for the total composite layer was found using Eq. 3.

$$\mu_{total}=\rho_{total}\,d_{total}=\rho_{SiN}\,d_{SiN}+2\rho_{Al}\,d_{Al}+\rho_{AlN}\,d_{AlN} \quad (3)$$

Tension in the composite structure was calculated from the fundamental flexural mode, verified by laser vibrometry.

Flexural modes were excited acoustically in each of the structures, and also excited electrically in the case of the structure with an AlN layer and top and bottom electrodes. Acoustic excitation was by a 1 MHz piezoelectric transducer transmitting through air. The 1 MHz transducer was excited off-resonance in the 10–300 kHz frequency range so that its resonant frequency was much higher than the natural flexural modes [1,1] to [3,3] of the devices under test in order to minimize its influence on the results. Displacement results were normalised by the measured response of the transducer. Electrical excitation was by a function generator connected between the upper and lower electrodes. The input voltage was 20–1000 mV and the frequency range was100–600 kHz. Laser vibrometry was used to record the out-of-plane displacement of the membrane, and by scanning across the membrane, surface displacement maps could be produced. The displacement value was taken as the peak-to-peak of the sinusoidal displacement which results in rectification of the observed modes.

## 3 Experimental results

Acoustic excitation experiments were carried out on the two bare $Si_3N_4$ membrane samples. Surface displacement maps for the 3.6×3.6 $mm^2$ $Si_3N_4$ membrane are shown in Fig. 2 and compared with analytical simulations. In this large membrane the multiple nodes and antinodes of the [1,1], [2,2] and [3,3] resonant modes can be clearly identified within the available frequency range and correspond well to the simulations. A frequency sweep 10–250 kHz was carried out and the displacement measured at a single point, approximately in the centre of the membrane. The resulting graph of displacement against frequency (Fig. 3) shows peaks which can be identified as the [1,1], [1,3] and [3,3] modes. Analytical simulations gave the following frequencies for the resonant modes: [1,1] 83, [1,2] 131, [2,2] 166, [1,3] 185, and

Table 1 Material properties

| | Membrane $Si_3N_4$ | Bottom electrode Al | Active layer AlN | Top electrode Al | Total layers composite |
|---|---|---|---|---|---|
| Thickness, d [nm] | 300 ±10 | 100 ±20 | 3000 ±500 | 100 ±20 | 3500 ±800 |
| Density, ρ [$kgm^{-1}$] | 2940[8] | 2700 | 3260 | 2700 | 3202 |
| Young's modulus, E [$GNm^{-2}$] | 289[8] | 70[9] | 345 at 25°C | 70[9] | – |
| Poisson's ratio, υ | 0.20[8] | 0.33 | 0.22 | 0.33 | – |
| Density area, μ [$kgm^{-2}$] | 0.0009 | 0.00003 | 0.009 | 0.00003 | 0.011 ±0.003 |
| Tension, T [$Nm^{-1}$] | 30 | 24[9] | 306[10] | 24[9] | 107 |

[3,3] 248 kHz. The [1,2] and [2,2] modes are expected to have antinodes at the centre of the membrane, therefore it is not possible to identify them on the frequency sweep.

A different investigation was made on the 400×400 μm$^2$ membrane, where the resonant frequencies were expected to be rather higher than for the large 3.6×3.6 mm$^2$ membrane. Thus only lower order modes could be excited acoustically using our experimental set-up. Figure 4(a) shows the evolution with frequency of the displacement measured along a diagonal scan of the membrane, corner to corner. At lower frequencies, a single peak is seen, splitting into two for the higher frequency modes. This demonstrates the evolution with increasing excitation frequency from the [1,1] mode at 580 kHz to the next resonance which corresponds to the degenerate [1,2] and [2,1] modes. Figure 4(b) shows 2-D spatial mapping at 920 kHz. At this frequency the degenerate [1,2] and [2,1] modes add coherently to give two diagonally opposite peaks. This result was also confirmed by analytical simulation. Electrical excitation with simultaneous laser vibrometry measurement of the out-of-plane displacement was carried out for the membrane device with an AlN layer and top and bottom electrodes. In Fig. 5 peaks can be seen corresponding to excitation of the [1,1] and [1,3] flexural modes. Amplitude of the modes increases with excitation voltage.

## 4 Discussion

Analytical and experimental results from the membrane devices were compared by matching the frequencies of the resonant modes. The most difficult parameter to estimate was the tension in the composite membrane, therefore this was obtained experimentally by identifying one of the modes and using it to calculate *T*, which could then be used to calculate subsequent flexural modes using the analytical equation. Good estimates for other modes were made for the 400×400 μm$^2$ $Si_3N_4$ membrane, with and without AlN layers, based on identification of the [1,2] mode at 920 kHz and the [1,1] mode at 173 kHz as highlighted in italics in Table 2.

Further investigation was carried out by simulation of the influence of intrinsic materials parameters on the flexural modes of a membrane-based device, in particular the stress in the $Si_3N_4$ membrane and AlN layer. The CoventorWare Architect software simulation tool was used.

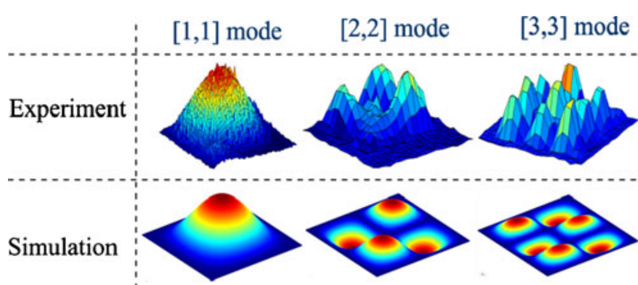


Fig. 2 Top, experimental 2-D mapping using scanning laser vibrometry of 3.6×3.6 mm$^2$ $Si_3N_4$ membrane. Bottom, corresponding calculated eigenmodes at 82 kHz [1,1], 165 kHz [2,2], and 248 kHz [3,3]

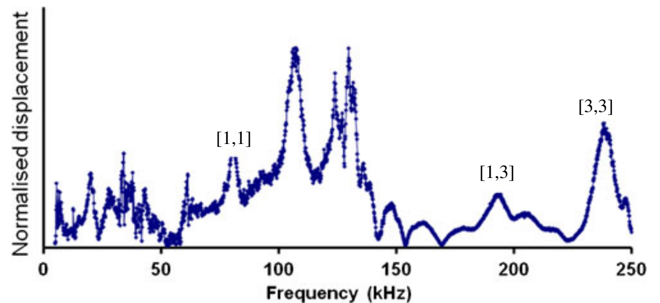


Fig. 3 Point displacement measurement for a frequency sweep 10–250 kHz, approximately in centre of 3.6×3.6 mm$^2$ $Si_3N_4$ membrane. Excitation by air-coupled ultrasonic transducer driven off-resonance

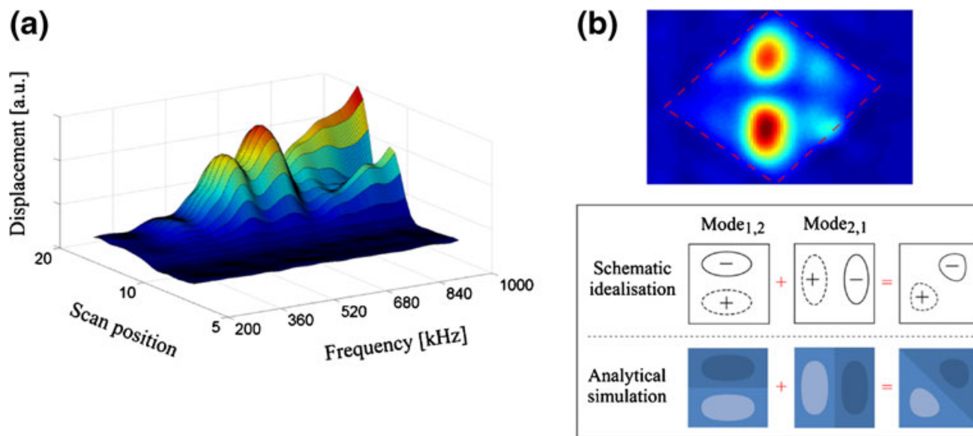


**Fig. 4** Spatial mapping of resonant modes of 400×400 μm² $Si_3N_4$ membrane. (**a**) Displacement of membrane scanned corner to corner for different frequencies of excitation transducer. (**b**) Top, 2-D surface scan at 920 kHz showing two diagonally opposite peaks. Bottom, superposition of [1,2] and [2,1] modes leads to the cancellation of zones of opposite sign, as shown in schematic diagrams and analytical simulations

Simulations for the bare membrane showed an increase of the eigenmode frequencies with residual stress in the $Si_3N_4$ as it was varied from 0 to 100 MPa, with the [1,1] mode varying from 40 to 350 kHz. This range of residual stress includes typical values obtainable from low stress LPCVD $Si_3N_4$ films as used here. For the composite membrane, the residual stress in the AlN film has a much larger effect than the stress in the $Si_3N_4$, mainly due to the larger layer thickness. For example, at typical values for the compressive stress magnitude in the AlN layer, a 20% variation in the resonant frequency was found by varying the stress in the $Si_3N_4$ membrane over the 0–100 MPa range. Further analysis with Architect could be used to estimate the residual stress in the AlN. Previous work on modal frequencies in FBAR resonators [11, 12] also showed that stress causes a shift in the resonant frequency of the device. Other effects on the normal mode frequencies in membrane structures include air loading (usually dominant in thin membranes [7]) and stiffness to bending and shearing (thick membranes).

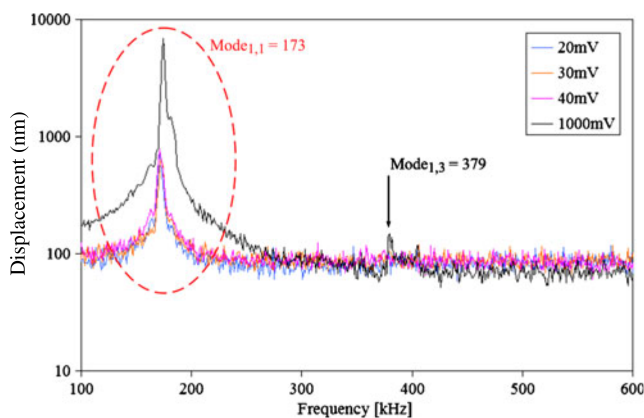


**Fig. 5** Electrical excitation of membrane structure with AlN layer at 20, 30, 40 and 1000 mV by sweeping the frequency over the range 100–1000 kHz. The [1,1] mode is visible at 173 kHz, and the [1,3] mode at 379 kHz for larger excitation voltage

## 5 Conclusions

The aim of this work was to investigate flexural modes in membrane structures incorporating AlN piezoelectric films and to characterise their acoustic resonances and electro-acoustic behaviour. We have shown that the flexural modes of a structure incorporating an AlN piezoelectric layer could be excited electrically or acoustically by using 2D mapping with a laser vibrometer to confirm the mode shapes. The analytical approach to calculating the mode shape was found to be adequate to determine vibrational modes of the samples, and was supplemented with more advanced MEMS modelling to investigate the effect of stress in the membrane and AlN layers.

Experimental values for resonant frequency were compared with analytical results and show that the approach used here is reliable. Scanning laser vibrometry is an important method of verifying the resonant modes. In the bare $Si_3N_4$ membrane, intrinsic stress in the membrane is significant. It was also found that the residual stress in the AlN active layer strongly affects the resonant frequency because it is much thicker than the other layers of the structure. Even with non-optimised electrode design it was possible to generate electrical excitation of the acoustic vibrational modes. The next step will consist in optimising

**Table 2** Flexural modes from analytical and experimental results for 400×400 μm² membrane structures with and without AlN active layer

| $Si_3N_4$ membrane, acoustic excitation | | AlN membrane structure, electrical excitation | |
|---|---|---|---|
| Analytical | Experimental | Analytical | Experimental |
| $Mode_{1,1}$=582 kHz | $Mode_{1,1}$=562 kHz | *$Mode_{1,1}$= 173 kHz* | *$Mode_{1,1}$= 173 kHz* |
| *$Mode_{1,2}$= 920 kHz* | *$Mode_{1,2}$= 920 kHz* | $Mode_{1,2}$=273 kHz | $Mode_{1,3}$=379 kHz |
| $Mode_{2,2}$=1,164 kHz | | $Mode_{2,2}$=346 kHz | |
| $Mode_{1,3}$=1,301 kHz | | $Mode_{1,3}$=386 kHz | |
| $Mode_{3,3}$=1,746 kHz | | $Mode_{3,3}$=518 kHz | |

the device for electrical response to mechanical excitation and quantifying the charge generation during flexion.

## References


1. Tirole, N., Choujaa, A., Hauden, D., Martin, G., Blind, P., Froelicher, M., Pommier, J.C., and Cachard, A., Lamb Waves Pressure Sensor using an AlN/Si Structure, IEEE Ultras. Symp., 371–374 (1993)
2. Piazza, G., Stephanou, P.J., and Pisano, A.P., Piezoelectric Aluminium nitride vibrating contour-mode MEMS resonators, J. MEMS, **15**(6), (2006)
3. Muralt, P., Ledermann, N., Baborowski, J., Barzegar, A., Gentil, S., Balgacem, B., Petitgrand, S., Bosseboeuf, A., and Setter, N., Piezoelectric micromachined ultrasonic transducers based on PZT thin films, IEEE Trans. Ultras. Ferroelect. Freq. Contr., **52**(12), (2005)
4. McRobbie, G., Wu, Z., Cochran, S., and Clark, F., Solutions to the silicon nitride problem, 11th Int. ANSYS Users Conf., (2004)
5. S.P. Beeby, M.J. Tudor, N.M. White, Energy harvesting vibration sources for microsystems applications. Meas. Sci. Technol. **17**, R175–R195 (2006)
6. McRobbie, G., Ling, Z., Wu, Z., Cochran, S., and Clark, F., Solutions to the vibrating membrane problem, Proc. 11th International ANSYS Users Conf. (Apr. 2004)
7. T.D. Rossing, N.H. Fletcher, *Principles of Vibration and Sound* (Springer, New York, 1995)
8. P. Khan, J. Philip, P. Hess, Young's modulus of silicon nitride used in scanning force microscopes cantilevers. J. Appl. Phys. **95**(40), 1667–1672 (2004)
9. K. Tanaka, K. Ishihara, Y. Akinaya, H. Ohta, Residual stress of aluminium thin films measured by X-ray and curvature methods. Mat. Sci. Res. Intern. **2**(3), 153–159 (1996)
10. Lapp, S., MSc thesis, University of the West of Scotland, 2006
11. Larson III, J.D., Ruby, R.C., Telschow, K.L., Observation of flexural modes in FBAR resonators at MHz frequencies, IEEE Ultras. Symp., 88–91 (2003)
12. M. Držík, H. Löschner, E. Haugeneder, W. Fallman, P. Hudek, I.W. Rangelow, Y. Sarov, T. Lalinský, J. Chlpík, Mechanical characterisation of membrane like microelectronic components. Microelec. Eng. **83**, 1036–1042 (2006)